Nuclear Data for Science and Technology (1988 MITO), 299- 302, Copyright © 1988 JAERI.

FUSION PRODUCT SPECTRA

Thurman L. Talley and Gerald M. Hale

Theoretical Division
Los Alamos National Laboratory
Los Alamos, New Mexico, USA

Abstract: Accurate fusion product data is required for most fusion plasma simulations. The energy broadening of reaction products is demonstrated to be more complicated than the usual Gaussian broadening. The accurate integrals are performed to obtain $\langle E_{incoming}\rangle$, $\langle\sigma v\rangle$, and $\langle\frac{dN}{dE}\rangle$ for all binary reactions in the four- and five-nucleon systems. Reaction cross sections were developed using R-Matrix models[1] that include most recent measurements.[2]

(Keywords: Thermal-Averaged, Fusion, Spectra)

Introduction

In addition to specific reactivity, $\langle\sigma v\rangle$, other Maxwellian averaged quantities are useful in fusion simulation. Fusion product spectra determine the energy deposition ranges and times. A general expression is developed for the averaged energy spectrum, $\langle\frac{dN}{de}\rangle$, and a tabulation is made for four and five nucleon fusion reactions.[1,2] This tabulation also includes $\langle\sigma v\rangle$ and $\langle E_{incoming}\rangle$ (more precisely $\frac{\langle\sigma ve\rangle}{\langle\sigma v\rangle}$), the reaction averaged incoming relative energy

Average Fusion Spectrum

A general differential or distribution function for specific reactivity for the reaction (1) + (2) $\xrightarrow{Q}$ (3) + (4) is

$$d^{12}N = f_c(E_c)f_r(e)\frac{2ede}{\mu^2}\sqrt{\frac{2E_c}{M}}\frac{dE_c}{M}\,d\hat{\Omega}_r\,d\hat{\Omega}_c\frac{d\sigma}{d\Omega_r'}\,d\hat{\Omega}_r'$$

$$\cdot\,\delta(\hat{\Omega}_c'-\hat{\Omega}_c)\,d\hat{\Omega}_c'\,\delta(E_c'-\frac{M}{M'}E_c)dE_c'\,\delta(e'-e-Q)de' \quad (1)$$

where $M = m_1+m_2$ = total mass, incident

$M' = m_3+m_4$ = total, mass, exit

$E_c = \frac{MV^2}{2}$ = CM incident energy

$E_c' = \frac{M'V'^2}{2}$ = CM exit energy

$M\underline{V} = m_1\underline{v}_1+m_2\underline{v}_2 = M'\underline{V}'=m_3\underline{v}_3+m_4\underline{v}_4$=momentum

$\mu = \frac{m_1m_2}{M}$, $\mu' = \frac{m_3m_4}{M'}$, reduced masses

$\underline{v} = \underline{v}_1 - \underline{v}_2$, $\underline{v}' = \underline{v}_3 - \underline{v}_4$, relative velocities

$e = \frac{\mu v^2}{2}$, $e' = \frac{\mu' v'^2}{2}$, relative energies

$e' = e + Q$, reaction energy production

$\hat{\Omega}$ = unit angle vector; $d\Omega_c = d(\cos\theta_k)d\phi_k$

$\theta \equiv kT$ = plasma energy

$f_c(E_c) = (\frac{M}{2\pi\theta})^{3/2}\exp(-\frac{E_c}{\theta})$ CM Distribution

$f_r(e) = (\frac{\mu}{2\pi\theta})^{3/2}\exp(-\frac{e}{\theta})$ Relative Distribution

$\frac{d\sigma}{d\Omega_r'}$ = differential cross section (angular distribution) for outgoing particle into $d\hat{\Omega}_r'$ measured from $\hat{\Omega}_r$.

δ = Dirac delta functions to conserve momentum and energy.

Direct integration of Eq. (1) gives $\langle\sigma v\rangle$ but to obtain an outgoing spectrum in the lab frame, it is necessary to transform from E_c' and ε' to the desired outgoing lab energy, say E_3. Kinematics give

$$M'E_3 = m_3E_c' + m_4e' + 2\beta\sqrt{m_3E_c'}\sqrt{m_4e'} \quad (2)$$

where $\beta = \hat{\Omega}_c'\cdot\hat{\Omega}_r'$.

Making this transformation (say, E_3 for E_c') and performing the analytic integrals, one may obtain (after much work)

$$\langle\frac{dN}{dE_3}\rangle = \frac{\sqrt{2}}{\pi}\frac{M'^{3/2}}{\sqrt{m_1m_2m_3m_4}}\int_0^\infty\frac{de}{\theta^2}\frac{e\sigma(e)}{\sqrt{e+Q}}\left[\exp(-J^-)-\exp(-J^+)\right] \quad (3)$$

where $J^\pm = \frac{e}{\theta}+\frac{M'}{Mm_3\theta}\left[\sqrt{M'E_3}\pm\sqrt{m_4(e+Q)}\right]^2$

A confirmation of (3) is that, when it is integrated over E_3, the resulting expression is the usual form for $\langle\sigma v\rangle$. The remaining integral in (3) must be performed numerically in general.

Computation

The STEEP4 code[3] was modified to evaluate the average of Eq. (3). Dense trapezoid integration assured minimal numeric errors. A tabulation at 120 plasma energies (θ) from 0.2 to 1000 keV and seven (7) points uniform in $\sqrt{E_3}$ for each plasma energy has been made. A numerical integration (Gaussian/Maxwellian interpolation/extrapolation) over E_3 for all the tabulation gives an error estimate when compared with $\langle\sigma v\rangle$. The error is less than 10^{-6} for most plasma energies but becomes substantially larger at the 1-MeV plasma energy. Here the error ranges from less than 10^{-3} to a maximum of 0.008. The difficulty at the high energies is extrapolation of the high energy tail with only 7 points. More points could have been used but were not considered necessary for current purposes. The $\langle\frac{dN}{dE}\rangle$ are normalized to unity $\langle\sigma v\rangle$ in the tabulation.

At each plasma energy the tabulation also contains $\langle\sigma v\rangle$ and an average incoming relative energy per fusion reaction $\frac{\langle\sigma ve\rangle}{\langle\sigma v\rangle}$, which is called $\langle E_{incoming}\rangle$. The documentation[3] of STEEP4 fully analyses the errors in such averages.

Results

$\langle \frac{dN}{dE} \rangle$, $\langle \sigma v \rangle$, and $\langle E_{incoming} \rangle$ are tabulated for the four- and five-nucleon rections $^2H(d,n)^3He$, $^2H(d,p)^3H$, $^3He(n,p)^3H$, $^3H(p,n)^3He$, $^3H(d,n)^4He$, and $^3He(d,p)^4He$ that result from R-Matrix analyses.[1] Other reactions can be added as required by application. Plots are shown in Figs. 1-11

The DT neutron spectrum (Fig. 7) represents a case where the usual Gaussian spreading approximation is adequate, whereas the DD products (Figs. 1 and 3) and the n^3He proton (Fig. 5) illustrate a transition to a Maxwellian type shift to higher energies at the higher plasma temperatures. Figure 10 shows the light product distribution for an endothermic reaction. The dotted lines of that figure represent Maxwellian distributions at the plasma temperatures listed. The departure from Maxwellian is real and interesting.

Figure 11 shows $\langle E_{incoming} \rangle$ in solid lines with dotted lines representing the Gamow energy (E_{Gamow} -Q for the endothermic reaction). The error resulting from the use of E_{Gamow} varies from 10% at the low temperatures to a factor of 2 underestimate at the higher temperatures. When Q is very large compared with plasma energies, this error may still be unimportant. It is important for the DD reactions, however.

Tabular data is also available on a mailable floppy disk (IBM-PC DOS formatted) with accompanying documentation for those persons desiring to use the data represented in the figures.

References

1. G. M. Hale and D. C. Dodder, "R-Matrix Analyses of Light-Element Reactions for Fusion Applications," Nuclear Cross Sections for Technology, NBS 594 (1980).
2. R. E. Brown, N. Jarmie, and G. M. Hale, "Fusion Energy Reaction $^3H(d\alpha)$ at Low Energies, Phys. Rev. C 35, pp. 1999-2004 (June 1987).
3. D. R. Harris, et al., The STEEP4 Code For Computation of Specific Thermonuclear Reaction Rates from Pointwise Cross Sections," Los Alamos report LA-6344-MS (June 1976).

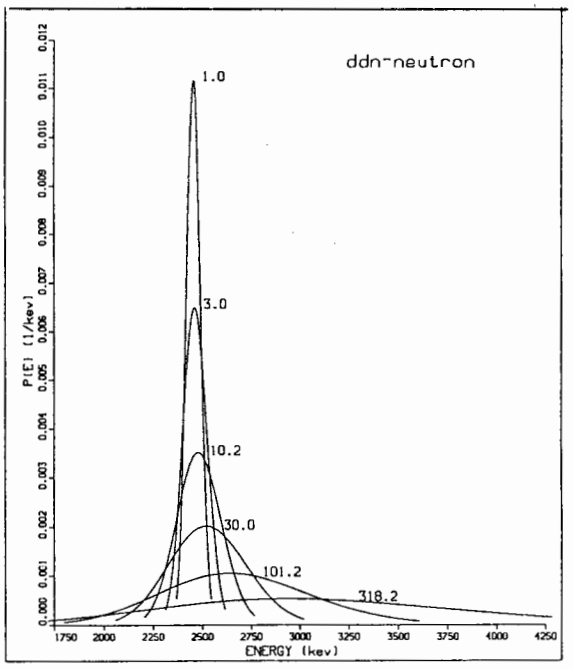

Fig. 1. Normalized $\langle \frac{dN}{dE} \rangle$ for the neutron from $^2H(d,n)^3He$. The labels are plasma temperatures (kT) for each curve.

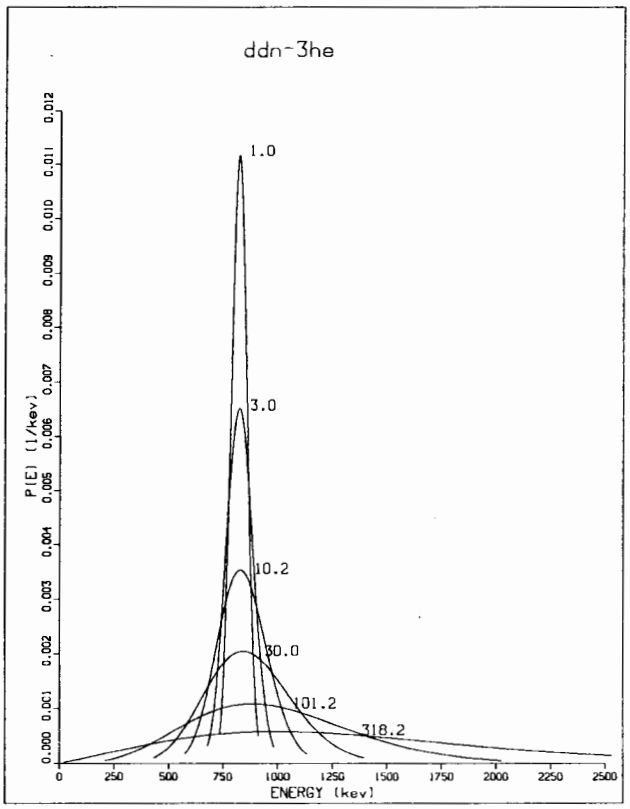

Fig. 2. Normalized $\langle \frac{dN}{dE} \rangle$ for the ^3He from $^2H(d,n)^3He$. The labels are plasma temperatures (kT) for each curve.

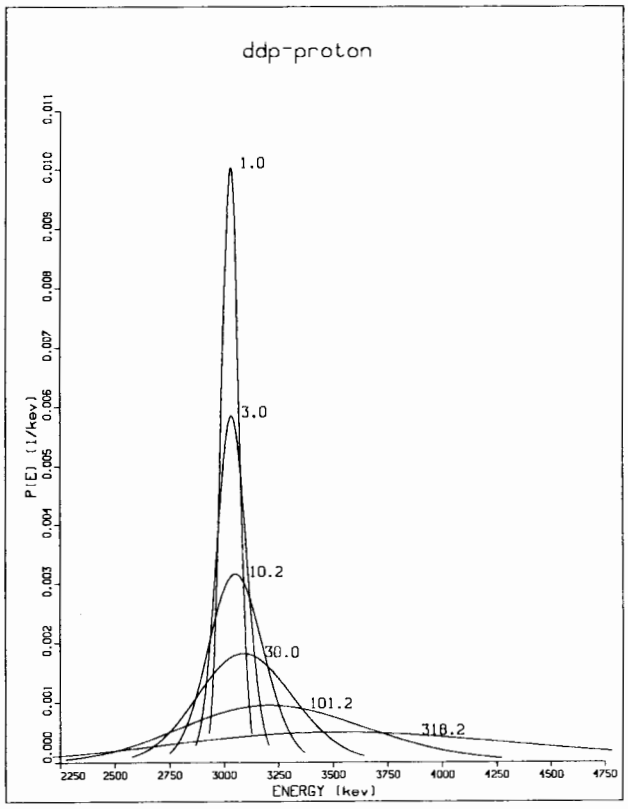

Fig. 3. Normalized $\langle \frac{dN}{dE} \rangle$ for the proton from $^2H(d,p)^3H$. The labels are plasma temperatures (kT) for each curve.

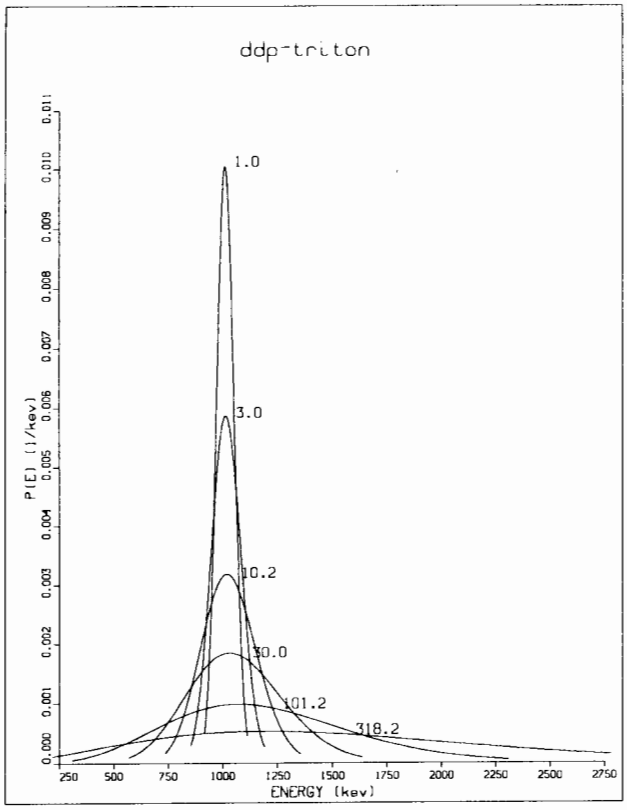

Fig. 4. Normalized $\langle \frac{dN}{dE} \rangle$ for the triton from $^2H(d,p)^3H$. The labels are plasma temperatures (kT) for each curve.

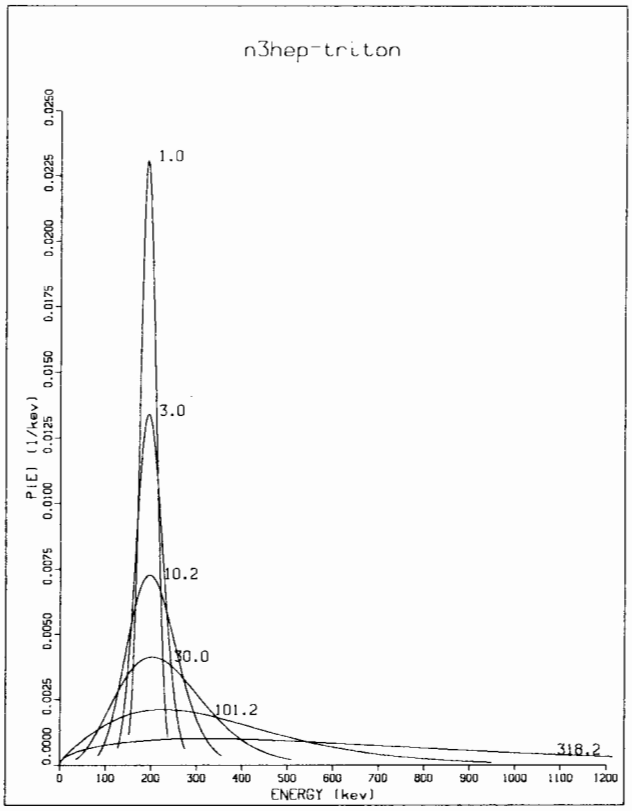

Fig. 6. Normalized $\langle \frac{dN}{dE} \rangle$ for the triton from $^3He(n,p)^3H$. The labels are plasma temperatures (kT) for each curve.

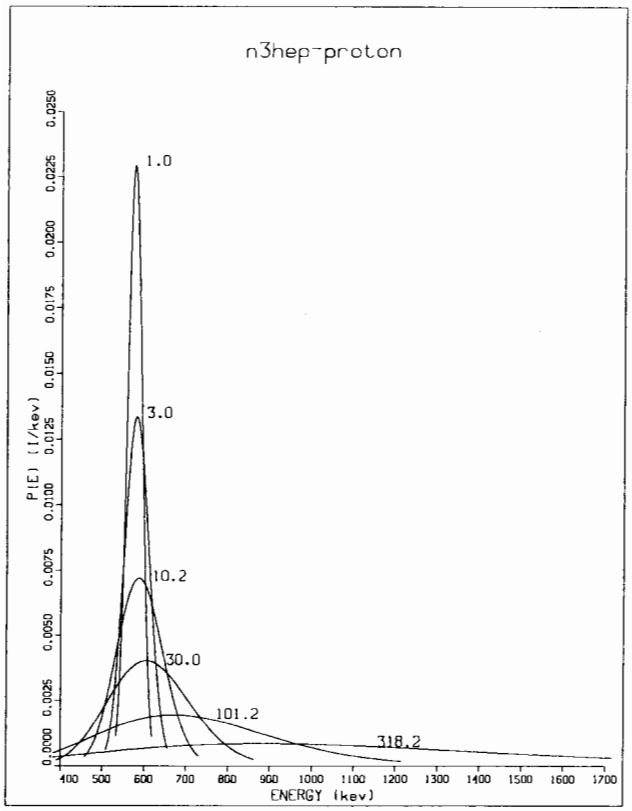

Fig. 5. Normalized $\langle \frac{dN}{dE} \rangle$ for the proton from $^3He(n,p)^3H$. The labels are plasma temperatures (kT) for each curve.

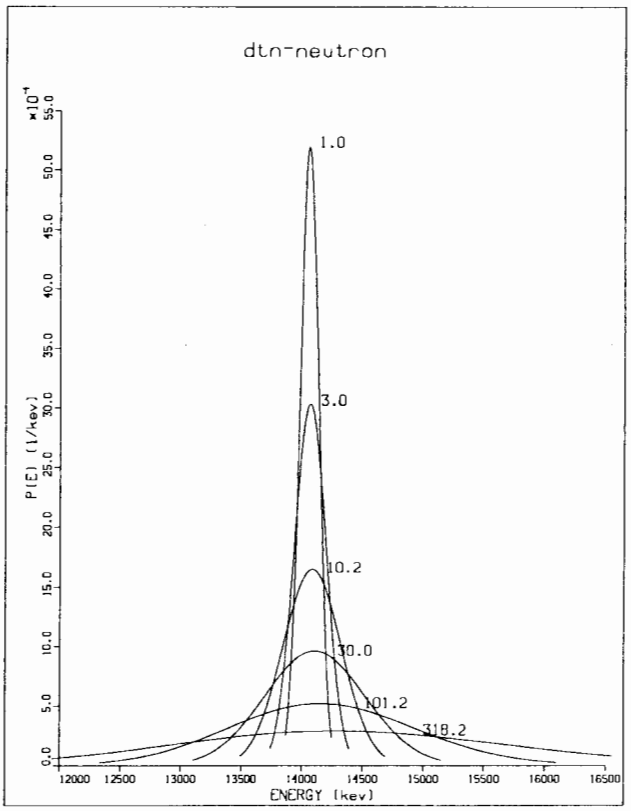

Fig. 7. Normalized $\langle \frac{dN}{dE} \rangle$ for the neutron $^3H(d,n)^4He$. The labels are plasma temperatures (kT) for each curve.

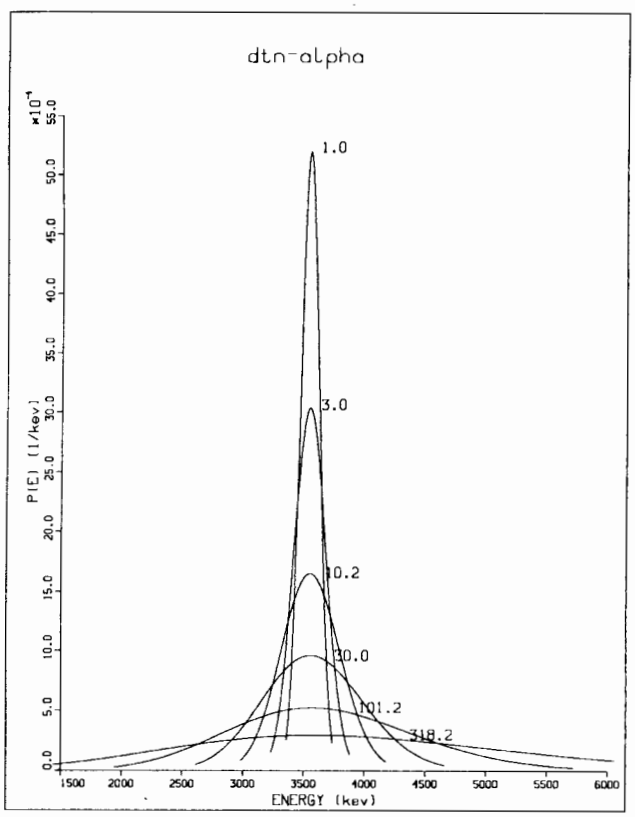

Fig. 8. Normalized $\langle \frac{dN}{dE} \rangle$ for the alpha from $^3H(d,n)^4He$. The labels are plasma temperatures (kT) for each curve.

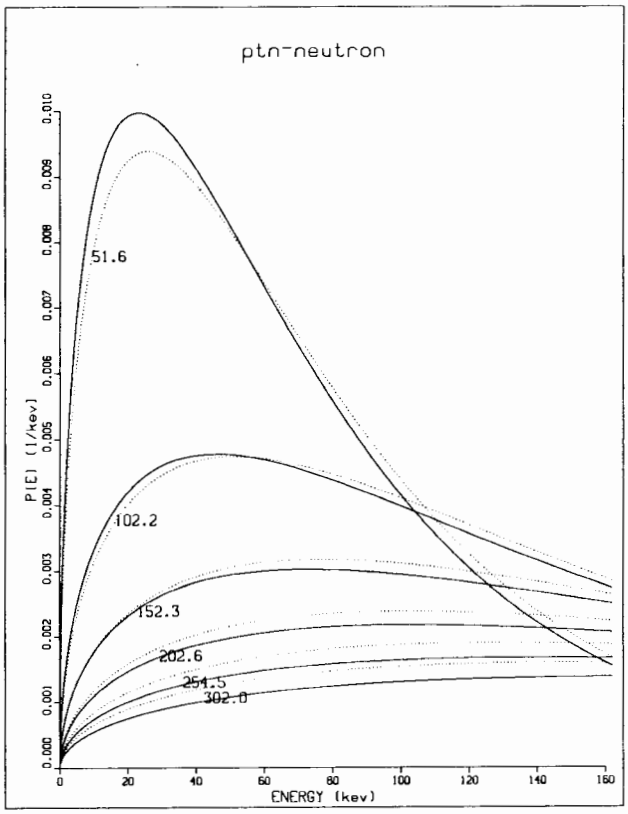

Fig. 10. Normalized $\langle \frac{dN}{dE} \rangle$ for the neutron $^3H(p,n)^3He$. The labels are plasma temperatures (kT) for each curve. The dotted lines are Maxwellian distributions at the listed temperatures.

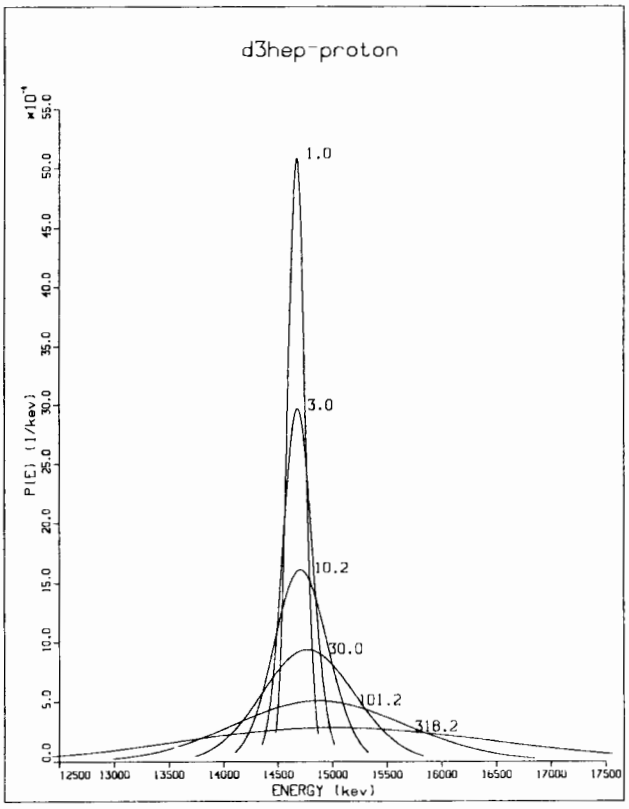

Fig. 9. Normalized $\langle \frac{dN}{dE} \rangle$ for the proton $^3He(d,p)^4He$. The labels are plasma temperatures (kT) for each curve.

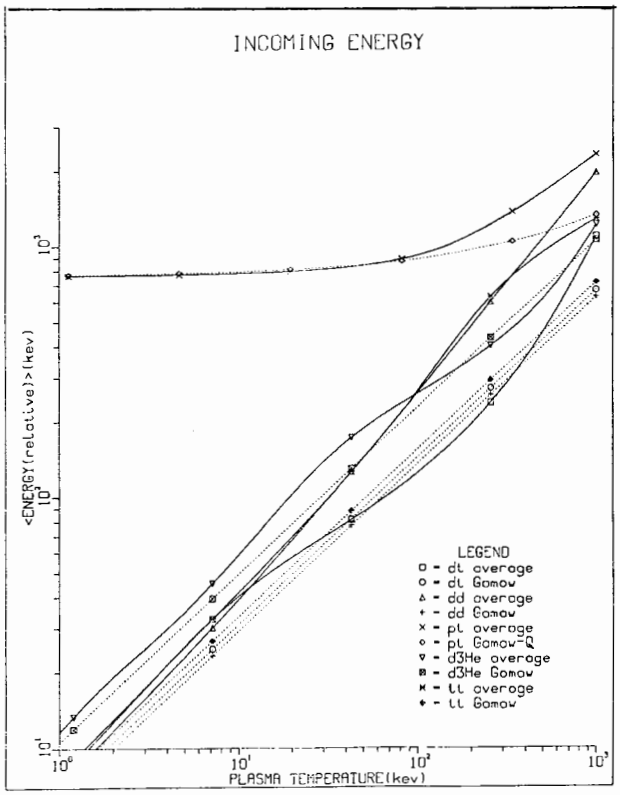

Fig. 11. Average incident relative energy of reacting nuclei as a function of plasma temperature (kT). The dotted lines represent Gamow energy plots for the reactions.